ChemTech

International Journal of ChemTech Research
CODEN (USA): IJCRGG, ISSN: 0974-4290, ISSN(Online):2455-9555
Vol.11 No.09, pp 298-307, 2018

Micro Structural Properties of Tin Doped Indium Oxide Thin Films

G. Ramanathan[1]*, K.R.Murali[2]

[1]Department of Physics, Sri Sairam Engineering College, Chennai, 600 044 India
[2]Department of Theoretical physics, University of Madras, Chennai, India.

Abstract : Tin doped Indium Oxide (ITO) thin films with different concentration of tin oxide (5%, 10%,70%) were prepared on glass substrate using dip coating sol gel method. The films were single phase with bixbyte structure. Micro structural parameters were determined from the XRD data. The crystallite size decreased with increase of tin concentration. From EDXA spectrum SnO_2 content were presented in the films with different percentage. Surface roughness increased from 0.20 nm to 1.25 nm as the tin concentration decreases. The films showed 85% transmission and transport properties of ITO were studied and these values are reported. The room temperature PL spectra of the samples formed at different concentration of SnO_2. From Raman spectrum the vibration mode appeared at 144,175 and 584 cm^{-1} in the ITO spectrum. These properties are suitable as transparent electrode for DSSC and sensors application.
Keywords : SnO_2 doped Indium oxide, thin films, sol gel, Transport properties, PL spectrum.

Introduction:

Transparent Conducting Oxide (TCO) films have been widely used for a variety of optoelectronic devices [1-2], energy efficient windows [3], Light Emitting Diodes (LEDs) [4-6] Flat Panel Displays (FPD) [7], and storage-type cathode ray tubes [7], solar cells [8], gas sensors [9], photo catalysts [10], and surface layers in electroluminescent applications [11]. Among the existing TCOs, Sn doped In_2O_3 (ITO) is one of the most frequently used material because of its unique characteristics such as low resistivity, high optical transmittance over the visible wavelength region, excellent adhesion to substrates and chemical stability. ITO is an n type semiconductor with a band gap between 3.5 and 4.3 eV at room temperature with bixbyte structure [12]. In order to obtain optimal characteristics, i.e. high transparency in visible region and high reflectance in near-IR region, parameters such as film thickness, substrate temperature, doping type and its amount, annealing temperature and the other deposition conditions have to be optimized. Surface coatings can be produced by variety of techniques such as evaporation [13], sol gel technique [14], pulsed laser deposition [15] and electron beam evaporation [16].Although several synthesis and processing methods have been employed for making thin-films of ITO, In this Paper ITO films deposited by the dip coating sol gel technique, and the results are reported.

G. Ramanathan *et al* /International Journal of ChemTech Research, 2018,11(09): 298-307.

DOI= http://dx.doi.org/10.20902/IJCTR.2018.110936

Experimental:

Tin doped Indium Oxide (ITO) thin films preparation was given in our earlier paper [17]. After preparation the films formed on the surface was dried in air oven for 15 min followed by different annealing temperatures (350 - 450 ^oC). The films thickness was measure by profilometer in the range of 450 nm to 950 nm with increasing temperature. Investigations of the microstructure were carried out an X-ray diffractometer. The surface morphology of the ITO films was examined by AFM. Optical transmission spectra, Photoluminescence studies and transport properties were studied by four probe method.

Result and Discussion:

Fig.1. shows the XRD patterns of the ITO films of different composition(5%,10%,70%) formed at different temperatures. The samples have the same cubic, bixbyite structure, of In_2O_3, (JCPDS 6-0416). Also, none of the spectra corresponding to higher annealing temperatures indicate any characteristic peaks of Sn, SnO, SnO_2, which indicates that the Sn atoms are probably incorporated substitution alloy into the In_2O_3 lattice [18,19]. Fig.2. shows the variation crystallite size verse % of SnO2 concentration, the mean crystallite size (38 nm) can be calculated by Debye's Scherer formula from the line broadening of the (2 2 2) reflection. It is good agreement with AFM observations, a progressive reduction of grains size has been found.

The lattice constant is observed to increase with the content of Sn^{4+} under the solubility limit. It is likely that the solute Sn^{4+} ions substitute at In^{3+} sites in the In_2O_3-SnO_2 solid solutions. Because the ionic radius of In^{3+} is 0.080 nm and that of Sn^{4+} is 0.069 nm [20], a slight increase in lattice constant by Sn^{4+} substitution appears to be somewhat counter-intuitive. However, it should be noted that Sn^{4+} has different valences than the host In^{3+} and charge compensation must be fulfilled during the Sn^{4+} substitution. The insertion of O_2^- in the vacant sites is one possible mechanism to compensate this charge unbalance. Insertion of O_2^- in the vacant sites will increase the lattice constant of the bixbyite structure because of the mutual repulsion between O_2^- ions, and thus the total lattice constant will be affected by the both Sn^{4+} substitution (contraction) and the O_2^- insertion (expansion) effects. The slight increase in lattice constant by Sn^{4+} addition in In_2O_3- SnO_2 solid solution supports the charge compensation by the O_2^- insertion into O vacancy sites during the Sn^{4+} substitution to the In^{3+} sites. The crystals defect parameters like microstrain and dislocation density show a decreasing trend with decrease in tin concentration. At low tin concentration, both the microstrain and dislocation density are minimum, which reveals the reduction in the concentration of lattice imperfections leading to preferred orientations [13]. The microstrain and dislocation density were calculated using the following relations.

$\beta\cos\theta/\lambda = 1/D + \varepsilon \sin\theta/\lambda$ ---------------(1)

The plot of $\beta\cos\theta/\lambda$ vs$\sin\theta/\lambda$ allows us to determine strain (ε) from slope of the graph. The dislocation density (δ) was obtained from the following relation

$\delta = 15\varepsilon /(aD)$ ----------------------------------(2)

The strain, lattice parameters, dislocation density and grain size are shown Table.1.

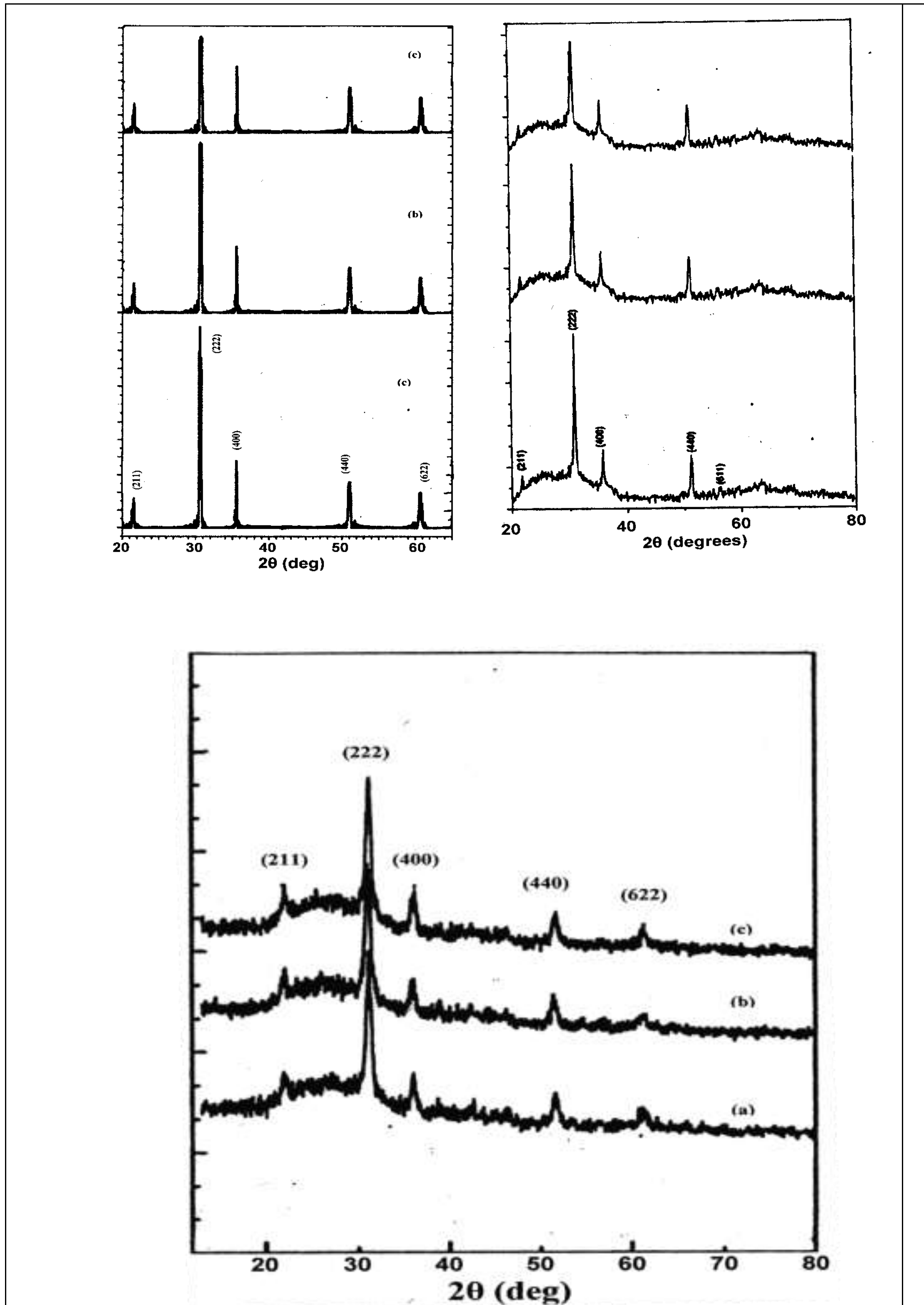

Fig.1. Shows X-ray diffraction pattern of 5 %, 10%, 70% tin oxide in ITO films formed at different temperatures (a) 350°C (b) 400°C (c) 450°C

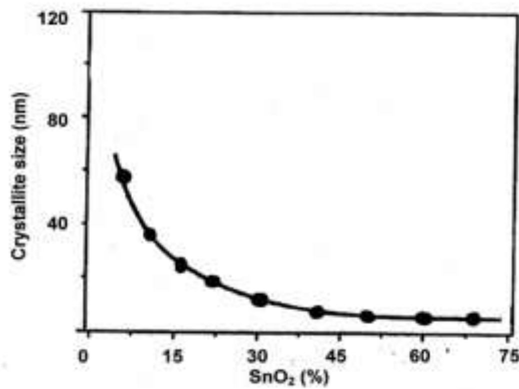

Fig.2. Shows Mean crystallite size with increase of tin concentration

The EDS spectra taken on samples of different composition are shown in figure.3 it confirms the presence of Indium, Tin, Oxygen elements and films thickness are listed in the table 2

Table – 1. Micro structural parameters of ITO films with different amounts of Tin oxide

Concen.of tin oxide (%)	Lattice parameters a (Å)	grain size (nm)	Strain (x 10^{-3})	Dislocation density 10^{13} lines m^{-1}
5	10.120	48	4.56	1.41
10	10.130	38	4.69	1.83
70	10.139	7	4.93	10.21

Table-2 shows atomic percentages of ITO films with different amounts of Tin oxide

%SnConcen.	Indium	Tin	Oxygen	Thickness (nm)
5	33.5	1.5	65	500
10	31.4	2.1	66.5	530
70	26	4.4	69.6	890

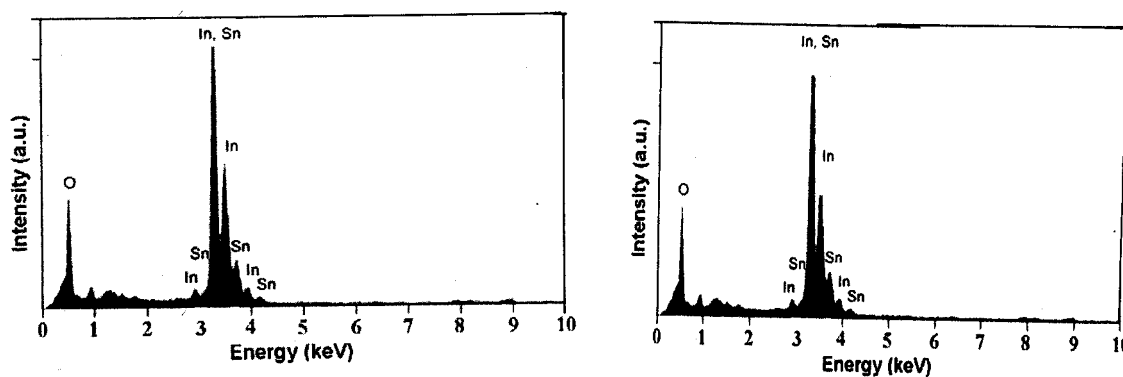

Fig.3. shows EDAX spectrum of ITO films (5 %, 70% SnO_2)

Fig.4.exhibits the Atomic Force Micrographs of ITO films formed at 450°C with different concentrations of tin. It is observed that the grain size decreases with increase of tin concentration. This is

supported by the XRD data. The surface roughness increases from 0.20 nm to 1.25 nm as the tin concentration decreases. The films are porous in nature. [21]

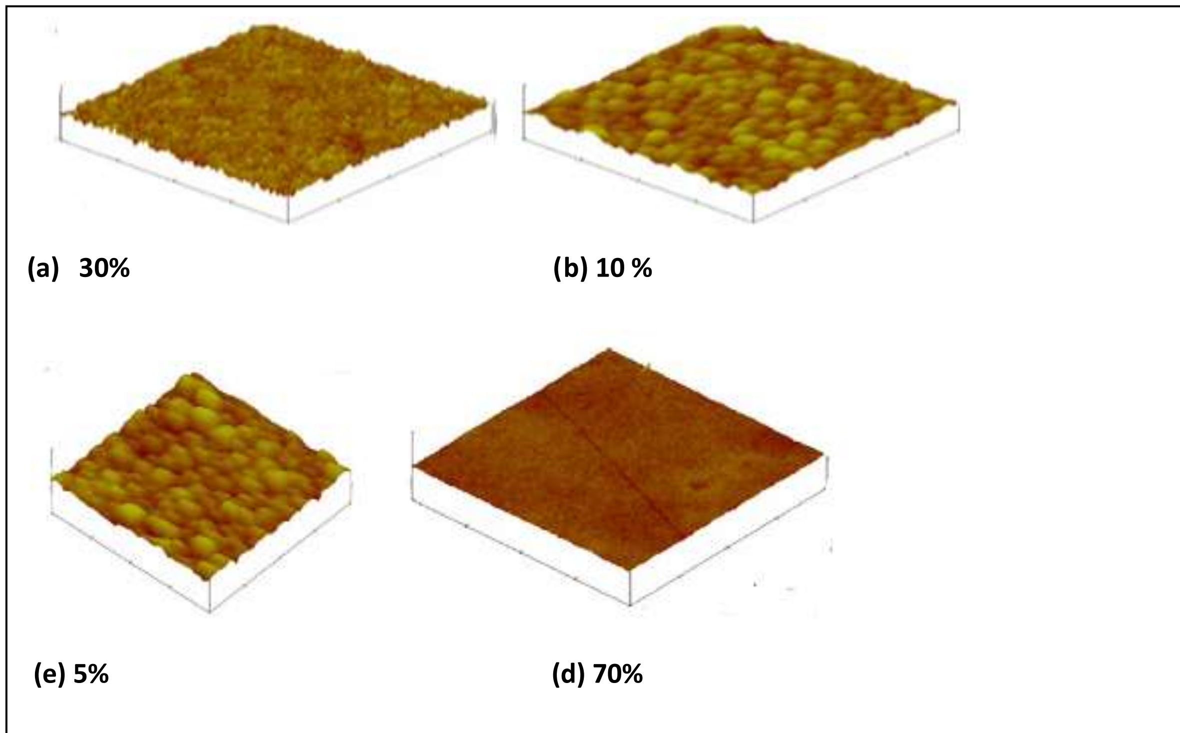

Fig.4, Shows Atomic Force Micrographs of ITO films with different concentrations of Tin formed at 450°C. (1 µm x 1 µm area). Z direction: 1 div – 5.0 nm

Fig.5.shows transmission spectra of ITO films formed at different Tin concentration. The transmittance of the films exhibits a sharp increase in the visible region. The ripples pattern seems to arise on account of interference of light which might be due to the characteristic of interference between light and nanostructure materials [22]. The transmission was found to be maximum for low SnO_2 concentration of In_2O_3 and decreased with an increase in SnO_2 concentration. The decrease in optical transmission is associated with the loss of light due to (i) Oxygen vacancies and (ii) Scattering at grain boundaries. Since all the films were deposited under similar oxygen environment and processing conditions, the loss of transmission due to oxygen defects was assumed to be same for all the deposited films. The increase in scattering centers due to more grain boundaries with an increase in Sn dopant content might be responsible for the loss of transmission. Thus a decrease in grain size with increase Sn concentration results in an increase in grain boundaries in In_2O_3 films.

The optical absorption coefficient, 'a' of a direct band gap semiconductor near the band edge, for photon energy hν greater than the band-gap energy E_g of the semiconductor, is given by the relation [23].$\alpha h\nu = A\,(h\nu - E_g)^{1/2}$ ------------------(3)

where h is Planck's constant and ν is the frequency of the incident photon. The Tauc plot of $(ah\nu)^2$ versus energy hν for the all ITO films were shown in Fig.5 The band gap energy was obtained by extrapolating the linear part of the Tauc plot curves to intercept the energy axis (at $\alpha h\nu = 0$). The estimated values of E_g for the ITO film were found to increase from 3.85 to 4.02 eV with an increase in Sn concentration in the In_2O_3 lattice. The allowed direct transitions were found previously for different ITO thin films and the direct optical band gap, E_g, values ranging from 3.5 to 4.5 eV were also reported earlier [19,24].

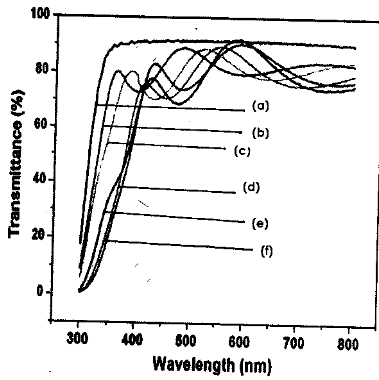

Fig.5 Shows Transmission spectra of ITO films with different concentrations of SnO_2 (a) glass (b) 5% (c) 10 % (f) 70 %

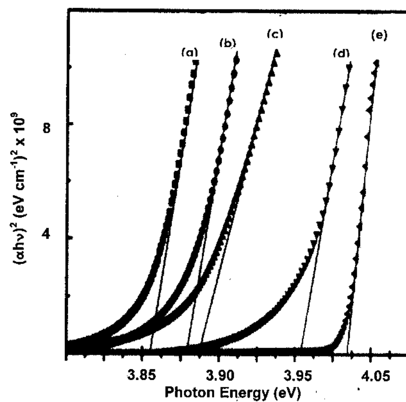

Fig.6. Tauc's plot of ITO films with different concentrations of tin oxide formed at 450°C (a) 5 % (b) 15 % (c) 30 % (d) 50 % (e) 70 %

Fig.6 shows the plot of refractive index as a function of wavelength λ for different percentages of SnO_2 in ITO films. The refractive index (n) was evaluated from the measured transmittance versus wavelength graph [25]. The refractive index was found to decrease with wavelength. It was observed that the refractive indices of the Sn-doped In_2O_3 thin films were smaller than for the pure In_2O_3 film in the measured wavelength range. The decrease in refractive index was attributed to the lowering in the value of grain size and increase in the porosity of the ITO film with the increase in Sn concentration

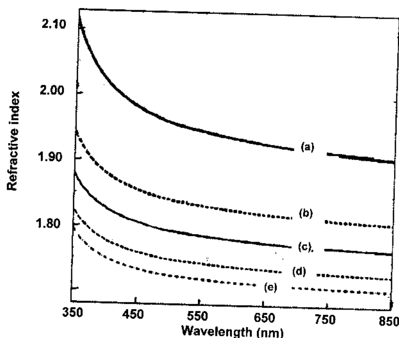

Fig.7. Variation of Refractive index with wavelength of ITO films formed at 450°C with different concentrations of Sn (a) 5 % (b) 10 % (c) 30 % (d) 50 % (e) 70 %

The resistivity of the films decreased from 20 ohm cm (In_2O_3 films formed at 450°C) to 0.1 ohm cm as the tin concentration increases to 10 %. Further increase of tin oxide content caused increased in resistivity. Beyond 10 % tin the resistivity increases from 0.1 ohm cm and attain 250 ohm cm .at 70 % tin concentration. The carrier density and mobility increase with increase of tin concentration up to 10 at. % beyond which, they decrease.The N_d increased from 1.61x 10^{20} cm^{-3} (In_2O_3 films formed at 450°C) to 1.25 x 10^{20} cm^{-3} up to 10 at. %, beyond this value of SnO_2 content, the carrier density decreases. The value of mobility decreased from 49.93 cm^2 $V^{-1}s^{-1}$ to 3.73 cm^2 $V^{-1}s^{-1}$ up to 10 at. % SnO_2, beyond which the mobility decreases. Fig.8. shows the variation of resistivity, mobility and carrier concentration with concentration of tin. The data are presented in table-3.The increase in resistivity beyond 10 % Sn can be explained as follows, this evolution could be described in terms of solubility of Sn atoms in the In_2O_3 lattice. As given in the literature [26], the maximum solubility of Sn-atoms in the In_2O_3 lattice is reached at approximately 10 at. %. So for an atomic concentration of Sn lower than 10 %, the Sn^{4+}ions substitute In^{3+} ions in the cationsublattice. As Sn^{4+} replace In^{3+}Sn atoms act as n-type donors, and the resistivity decreases with the Sn concentration. For higher tin content, no more Sn-atoms can be embedded in the In_2O_3-lattice, and the resistivity increases. This increase may be due to interstitial Sn-atoms in the lattice, which act as charged trapping centers for the electrons [27].

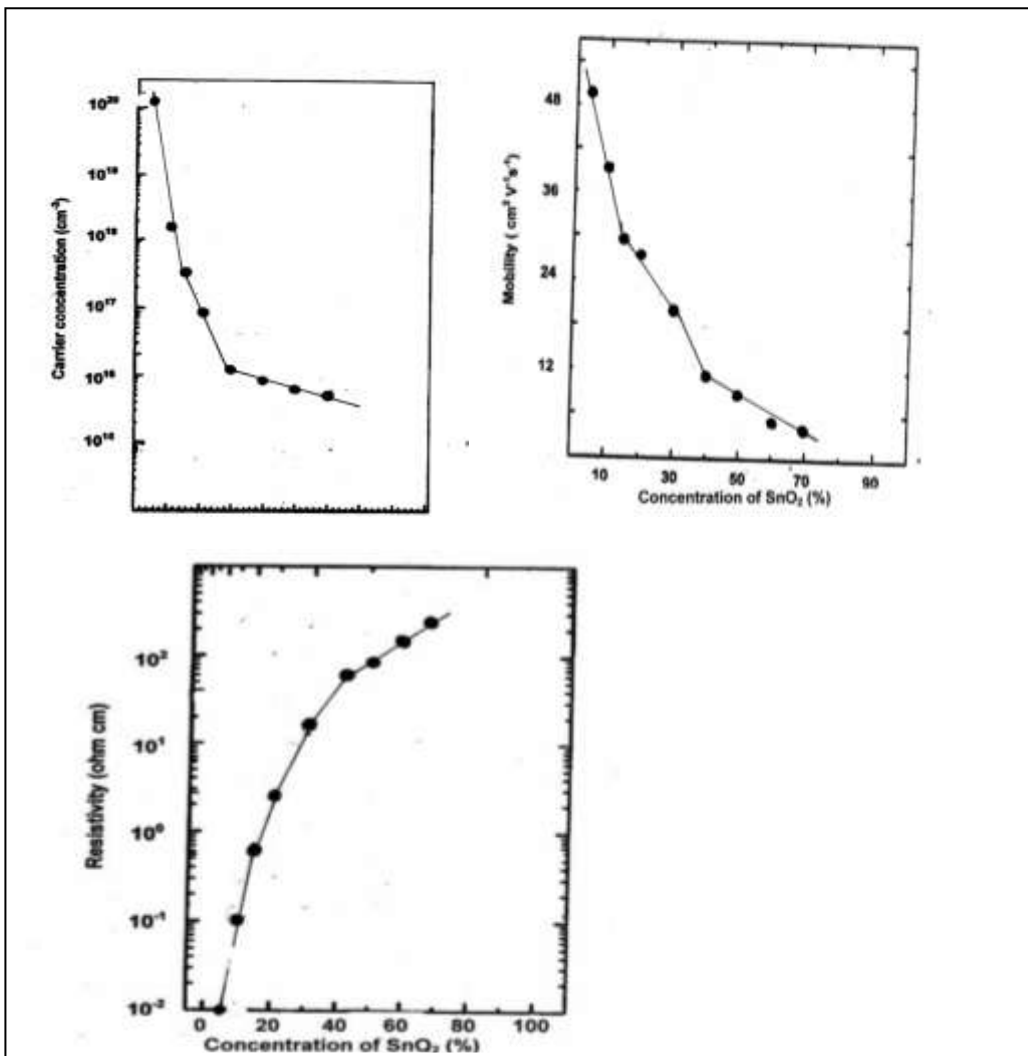

Fig.8. Shows the Variation of room temperature Resistivity, mobility and carrier concentration of ITO films with different concentration of SnO_2

Table -3 Transport parameters of ITO films with different Concentrations of Tin

Sn (at. %)	Resistivity (ohm cm)	Mobility ($cm^2V^{-1}s^{-1}$)	Carrier concentration (cm^{-3})
5	0.01	49.93	1.25 X 10^{20}
10	0.10	38.75	1.61 X 10^{18}
70	250.00	3.73	6.69 X 10^{15}

phase separation of SnO_2 in the crystalline ITO-material does not occur since no Bragg reflections belonging to a crystalline SnO_2 phase were detected for films with SnO_2 concentration up to 70 % in XRD measurements. Raman spectrum of undoped In_2O_3 shows vibrational modes at 109, 135, 307, 366, 495, 517 and 630 cm^{-1} which is an unambiguous signature of the cubic In_2O_3 structure [28]. These same features are readily observed in the ITO spectra, because the main contribution to the vibrational modes comes from the cubic In_2O_3 host lattice

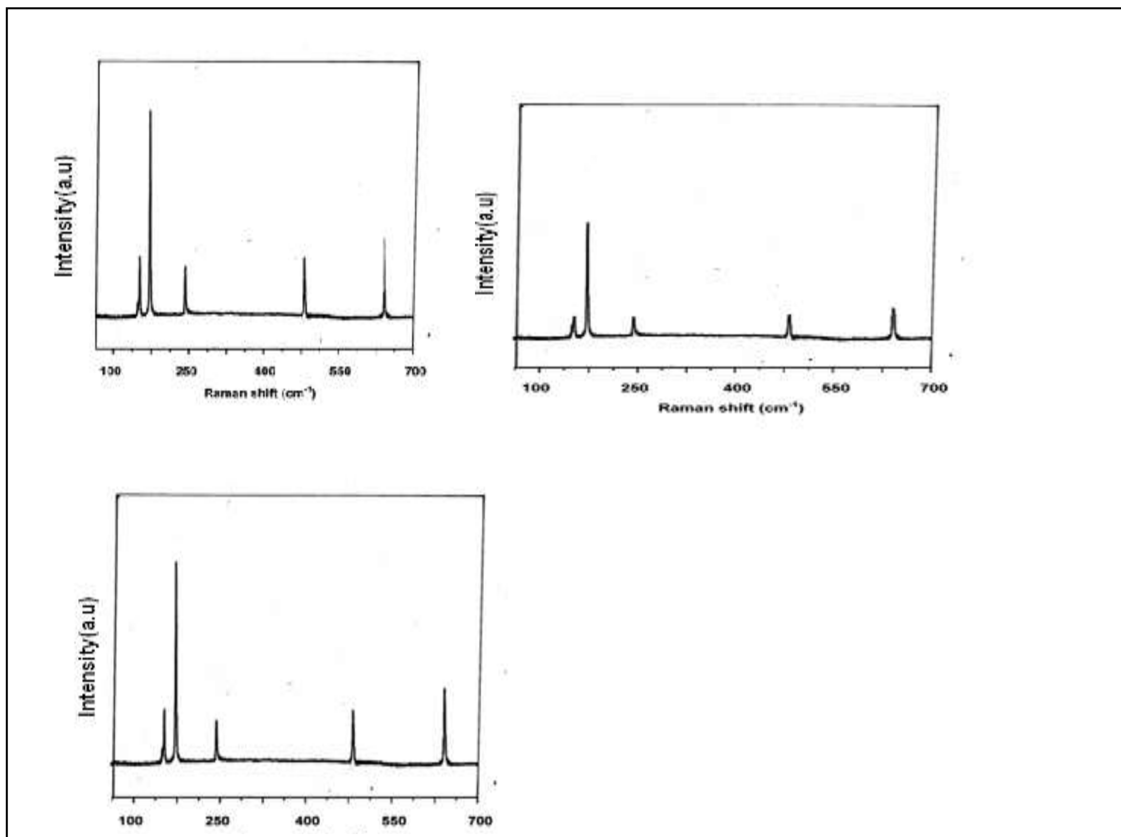

Fig.9. Shows room temperature Raman Spectrum of ITO films formed at 450°C with (5%,10%,70 %) tin oxide

The high frequency line in the ITO spectrum at 631 cm^{-1} is due to the superposition of the contribution of the In–O vibrational modes (630 cm^{-1}) and the Sn–O vibrational modes (633 cm^{-1}) in this work, vibration modes appeared at 144, 175 and 584 cm^{-1} in the ITO spectrum (Fig.9). These result matches with previous report [29]. The height of the peaks decreased as the tin oxide concentration increased. In fact the observation of these modes in the doped structure can be related to the Sn incorporation in the lattice. In this way, these modes can be indexed as Sn–O vibrations which make ITO distinguishable from the undoped material. Moreover, a narrow line width of Raman in all the spectra indicates that the films have a very good crystal quality.

The photoluminescence (PL) spectra (Fig. 10) of the films excited at the band gap energy (Eg = 4.0 eV, i.e.310 nm, λ_{ex}) of the excitons. Three PL bands appeared at 423, 486, 529 nm with a small broad peak at 439 nm. It is earlier reported [30, 31] that in the nanoclusters of semiconductors associated with defect centers,

emissions for both bound and free excitons wouldappear when kex is equivalent to Eg and emissions for only free excitons in the case λ_{ex} is $>$Eg or $<$Eg. Hence, we may predict that the PL bands at 423, 486 and 529 nm are for bound excitons trapped in the defect centers of ITO. The 439 nm band is possibly due to the defect of In–O vacancy [32].

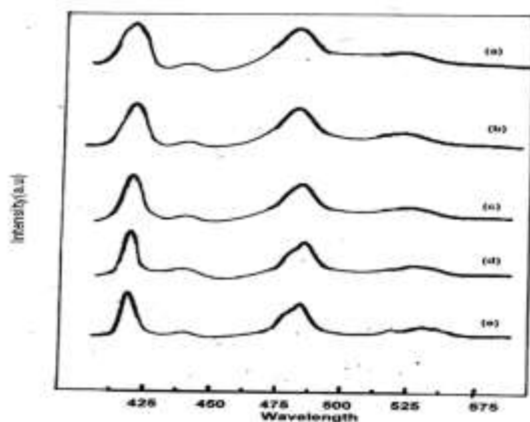

Fig.10. Room temperature photoluminescence emission spectra of ITO films containing different concentrations of Sn (a) 70 % (b) 60 % (c) 30 % (d) 20 %(e) 5 %

Conclusion:

The results of this work illustrate that single phase cubic, bixbyite structure of In_2O_3 films, grain size in the range of 7-48 nm can be deposited by dip coating sol gel method. Films with transmission in the range of 80-90% can be obtained. Thickness of the films varying from 500 nm to 890 nm. Low resistivity films can be obtained its band gap in the range of 3.85-4.02eV and with carrier density 1020 cm-3 can be deposited. Also this investigation clearly points to the possibility of using them solar cells and gas sensor applications.

References:

1. Parker D G P.G. Say, Electronics Letters, 22(1986)1266.
2. Andrade M C de ,Moehlecke S. Applied Physics A, 58 (1994) 503.
3. Hamberg, Granqvist C G , Berggren K F ,.Sernelius B E ,.Engstrom L, Vacuum, 35(1985)207
4. Lin Y C ,Chang S J, .Su Y K , Tsai T Y , Chang C S,.hei, S C et al. IEEE Photonics Technology Letters.14 (2002)1668.
5. Hagerott M, Jeon H, .Nurmikko A V, Xie W, Grillo D C,.Kobayashi M et al. Applied Physics Letters. V (1992) 2825
6. Kim H , Pique A, Horwitz J S, Mattoussi H , Murata H, Z.H.Kafafi Z Het al. Applied Physics Letters, 74(1999) 3444.
7. Pankove J I . Display devices. Berlin Heidelberg: Springer-Verlag; (1980)
8. Touskova J ,.Kovanda J, Dobiasova L, Parizek V , Kielar P. Solar Energy Materials and Solar Cells 37 (1995) 357.
9. Luff B J, Wilkinson J S, Perrone G, Applied Optics 36 (1997) 7066.
10. Poznyak S K, Golubev A N, Kulak A L, Surface Science 454(2000) 396
11. Tueta R, BraguieM , Thin Solid Films 80 (1981) 143.
12. Raoufi D,.Kiasatpour A. Allah H R,.Rosatian A S H, Applied Surface Science. 253 (2007) 9085.
13. De Carvalho C N,.doRego A M B,.Amaral A,.Broguerira P,.LavaredaG.Surface and Coating Technology, 70 (2000)124.
14. Alam M J , Cameron D C, Thin Solid Films, 377 (2000) 455
15. Adurodija F O, Izumi H,.Ishihara T, Yoshioka H, Yamada K, Matsui H et al.Thin Solid Films 79 (1999)350
16. Mori N , Ooki S,.MasubuchiN,.Tanaka A, Kogoma M, .Ito T, Thin Solid Films: 6. (2002)411
17. RamanathanG , John Xavier R , Murali K R ,IOSR journal Vol.2 issue 6 (2013) 47-50.

18. Fallah H R, GhasemiM ,Hassanzadeh A . Steki H, Mater. Res. Bull. 42 (2007) 487.
19. George J, Menon C S, Surf. Coat. Technol. 132 (2000) 45.
20. Shannon R D, Acta Crystallography. Sec. A 32 (1976) 751–767.
21. Ramanathan G, .Murali K R, International .J.Chem Tech Res. 8 (2015) 260-264.
22. Fallah H R, Ghasemi M, Hassanzadeh A, Physica E, 39(2007)69.
23. Hamberg I, . Granqvis C G, J.Appl.Phys.60 (1986) R123.
24. .Smith J F, .Aronson, A J Chen D, Class W,H, Thin Solid Films,72(1980) 469.
25. Swanepoel R, J Phys E, 17(1984) 896.
26. Frank G, Kostlin H, . Rabenau A, Phys.Stat. Solid A 52 (1979) 231.
27. Hamberg I, Granqvist C G, J.Appl.Phys.60 (1986) R123.
28. Sobotta H, Neumann H , uhn G K ,.Riede V, Cryst. Res. Technol. 25(1990) 61.
29. Kim D, Hwang I,.Kwon S J, Kang H, Park K,.Cho Yi, .Choi K, Park J, Nano Lett. 7(2007)3041.
30. Peng H Y, Lee C W,. Everit H O, Lee D S, SteckiA J,.Zavada J M, Appl. Phys. Lett. 86 (2005) 051110-1.
31. Nanda K , Sahu S N, Adv. Mater. 13 (2001) 280.
32. Wu X C , Hong X C Han Z.J , Tao Y.R , Chem. Phys. Lett. 373 (2003) 28.

*****